AIP | Applied Physics Letters

Achieving highly conductive AlGaN alloys with high Al contents

K. B. Nam, J. Li, M. L. Nakarmi, J. Y. Lin, and H. X. Jiang

Citation: Applied Physics Letters **81**, 1038 (2002); doi: 10.1063/1.1492316
View online: http://dx.doi.org/10.1063/1.1492316
View Table of Contents: http://scitation.aip.org/content/aip/journal/apl/81/6?ver=pdfcov
Published by the AIP Publishing

Articles you may be interested in
High p-type conduction in high-Al content Mg-doped AlGaN
Appl. Phys. Lett. **102**, 012105 (2013); 10.1063/1.4773594

Properties of N-polar GaN films and AlGaN/GaN heterostructures grown on (111) silicon by metal organic chemical vapor deposition
Appl. Phys. Lett. **97**, 142109 (2010); 10.1063/1.3499428

Si-doped high Al-content AlGaN epilayers with improved quality and conductivity using indium as a surfactant
Appl. Phys. Lett. **92**, 092105 (2008); 10.1063/1.2890416

Silicon doping dependence of highly conductive n -type Al 0.7 Ga 0.3 N
Appl. Phys. Lett. **85**, 4669 (2004); 10.1063/1.1825055

High-conductivity n-AlGaN with high Al mole fraction grown by metalorganic vapor phase deposition
Appl. Phys. Lett. **82**, 4289 (2003); 10.1063/1.1582377

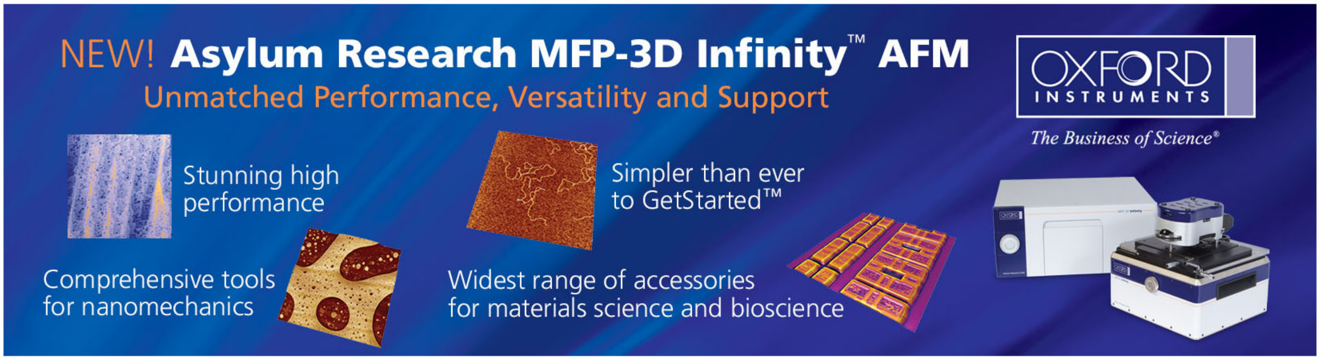

NEW! Asylum Research MFP-3D Infinity™ AFM
Unmatched Performance, Versatility and Support
Stunning high performance
Simpler than ever to GetStarted™
Comprehensive tools for nanomechanics
Widest range of accessories for materials science and bioscience
OXFORD INSTRUMENTS
The Business of Science®

This article is copyrighted as indicated in the article. Reuse of AIP content is subject to the terms at: http://scitation.aip.org/termsconditions. Downloaded to IP: 129.118.249.45 On: Fri, 02 May 2014 00:19:10

APPLIED PHYSICS LETTERS VOLUME 81, NUMBER 6 5 AUGUST 2002

Achieving highly conductive AlGaN alloys with high Al contents

K. B. Nam, J. Li, M. L. Nakarmi, J. Y. Lin, and H. X. Jiang[a]
Department of Physics, Kansas State University, Manhattan, Kansas 66506-2601

(Received 5 December 2001; accepted for publication 15 May 2002)

Si-doped *n*-type $Al_xGa_{1-x}N$ alloys were grown by metalorganic chemical vapor deposition on sapphire substrates. We have achieved highly conductive *n*-type $Al_xGa_{1-x}N$ alloys for x up to 0.7. A conductivity (resistivity) value of 6.7 Ω^{-1} cm^{-1} (0.15 Ω cm) (with free electron concentration 2.1×10^{18} cm^{-3} and mobility of 20 cm^2/Vs at room temperature) has been achieved for $Al_{0.65}Ga_{0.35}N$, as confirmed by Hall-effect measurements. Our experimental results also revealed that (i) the conductivity of $Al_xGa_{1-x}N$ alloys continuously increases with an increase of Si doping level for a fixed value of Al content and (ii) there exists a critical Si-dopant concentration of about 1×10^{18} cm^{-3} that is needed to convert insulating $Al_xGa_{1-x}N$ with high Al content ($x\geqslant0.4$) to *n*-type. © *2002 American Institute of Physics.* [DOI: 10.1063/1.1492316]

Currently, there is a great need of solid-state UV emitters for chem-bio-agent detections as well as for general lighting. In such applications based on III-nitride wide band gap semiconductors, highly conductive *n*-type AlGaN alloys with high Al contents are indispensable. $Al_xGa_{1-x}N$ alloys with high x are both very difficult to grow and to characterize due to their wide energy band gaps. Undoped $Al_xGa_{1-x}N$ alloys with high x ($x>0.4$) are generally insulating,[1,2] a fact that is directly correlated with a sharp increase of the carrier localization energy around $x=0.4$.[3] Previously, *n*-type $Al_xGa_{1-x}N$ (x up to 0.58) with a conductivity (resistivity) of about 0.08 Ω^{-1}cm^{-1} (13 Ω cm) has been obtained by Si-doping.[4] More recently, by employing indium–silicon codoping approach, an *n*-type conductivity of about 5 Ω^{-1}cm^{-1} has been obtained for $Al_{0.4}Ga_{0.6}N$ epilayers.[5] However, to obtain short wavelength emitters ($\lambda<300$ nm), highly conductive *n*-type $Al_xGa_{1-x}N$ alloys with Al contents as high as 0.6–0.7 are needed.

In this letter, we report our achievement of highly conductive $Al_xGa_{1-x}N$ alloys (x up to 0.7) by metalorganic chemical vapor deposition growth using Si-doping. Si-doped $Al_xGa_{1-x}N$ alloys (1 μm thick) were grown on sapphire (0001) substrates with AlN buffer layers. The growth temperature and pressure were around 1050 °C and 50 Torr, respectively. The metal organic sources used were trimethylgallium (TMGa) for Ga and trimethylaluminum (TMAl) for Al. The gas sources used were blue ammonia (NH_3) for N and Silane (SiH_4) for Si doping. The flow rates used for TMGa, TMAl, NH_3, and SiH_4 were about 3, 15, 2000, and 10 sccm, respectively. For $Al_xGa_{1-x}N$ alloys ($0.3\leqslant x\leqslant0.5$) with a fixed Al content, the doping level was varied, from which we concluded that a critical Si dopant concentration ($N_{Si}\sim1.0\times10^{18}$ cm^{-3}) is needed to convert insulating $Al_xGa_{1-x}N$ ($x>0.4$) to *n*-type. Highly conductive $Al_xGa_{1-x}N$ ($0.5\leqslant x\leqslant0.7$) alloys were then obtained by fixing the Si dopant concentration at 5×10^{18} cm^{-3} while varying the growth conditions slightly. The Al contents of Si-doped *n*-type $Al_xGa_{1-x}N$ alloys were determined by energy dispersive x-ray microanalysis and x-ray diffraction measurement as well as by the flow rates of TMGa and TMAl. The Al contents (x) determined by all three methods agreed within ±0.02. The Si-dopant concentrations were determined by the flow rate of SiH_4 as well as by the variable temperature Hall-effect measurement at elevated temperatures ($T<650$ K). Additionally, secondary ion mass spectroscopy measurements were performed (by Charles and Evan) for selective samples to verify the Si-dopant concentrations. Atomic force microscopy and scanning electron microscopy were employed to examine the surfaces and revealed crack-free $Al_xGa_{1-x}N$ epilayers. Variable temperature Hall-effect (standard Van der Pauw) measurements were employed to measure the electron concentration, mobility, and resistivity of these materials. A deep UV (10 mW@195 nm) picosecond time-resolved photoluminescence (PL) spectroscopy system was specially designed to probe the optical properties of materials and device structures based on $Al_xGa_{1-x}N$ alloys with high x and hence serves as ‘‘eyes’’ for monitoring the material qualities of these materials. The picosecond time-resolved PL spectroscopy system consists basically of a frequency quadrupled 100 femtosecond Ti: sapphire laser with a 76 MHz repetition rate, a monochromator (1.3 m), and a streak camera with a detection capability ranging from 185 to 800 nm and a time resolution of 2 ps.[6]

Table I summarizes the room temperature Hall-effect measurement results of the first batch of 25 $Al_xGa_{1-x}N$ samples ($0.3\leqslant x\leqslant0.5$). The general trends are that the conductivity of $Al_xGa_{1-x}N$ alloys increases with the Si dopant concentration (at a fixed value of x) and decreases with x (at a fixed value of N_{Si}). More detailed results for representative samples are discussed below.

Figure 1 presents the Si dopant concentration (N_{Si}) dependence of the room-temperature (300 K) PL spectra of three $Al_xGa_{1-x}N$ samples with $x=0.4$, 0.45, and 0.5. Besides the shift of the peak positions (E_p) toward longer wavelengths at higher doping levels due to the effect of the band gap renormalization, we also observe a considerable increase in the PL emission intensity with increasing N_{Si}. The improvement of optical quality by Si-doping has been observed previously in GaN epilayers[7–9] and GaN/AlGaN

---

[a] Author to whom correspondence should be addressed; electronic mail: jiang@phys.ksu.edu

0003-6951/2002/81(6)/1038/3/$19.00

TABLE I. Hall data of of Si-doped $Al_xGa_{1-x}N$ ($0.3\leqslant x\leqslant 0.5$) conductivity $(\Omega\,cm)^{-1}$ Hall mobility (cm^2/Vs)/Hall concentration (cm^{-3})

	x				
N_{Si} (cm^{-3})	0.3	0.35	0.4	0.45	0.5
0	7.32 12/3.81×10^{18}	0.47 23/1.29×10^{17}	5.2×10^{-3} 8.6/3.81×10^{15}	2.6×10^{-3} 3.1/5.30×10^{15}	High resistivity
5.0×10^{17}	0.4 9.6/2.60×10^{17}	0.49 11/2.80×10^{17}	0.16 4.8/2.11×10^{17}	0.21 4.9/2.3×10^{17}	0.23 5.2/2.81×10^{17}
1.0×10^{18}	0.62 13/2.99×10^{17}	4.5 36/7.82×10^{17}	0.67 10/4.17×10^{17}	0.13 4.2/1.92×10^{17}	0.013 3.1/2.66×10^{16}
2.5×10^{18}	15.3 61/1.57×10^{18}	21.0 56/2.35×10^{18}	15.4 60/1.60×10^{18}	4.85 37/8.19×10^{17}	**2.51** **16/9.82×10^{17}**
5.0×10^{18}	25.7 45/3.57×10^{18}	34.2 62/3.45×10^{18}	10.0 19/3.16×10^{18}	**10.2** **28/2.28×10^{18}**	0.88 14/3.94×10^{17}

multiple quantum wells.[10] The relative PL intensities for Si-doped $Al_xGa_{1-x}N$ alloys seen here increase by about one order of magnitude when the Si dopant concentration is varied from 0 to 5×10^{18} cm^{-3}. For example, for $x=0.45$, the relative PL emission intensity increases from 5 to 37 and to 44 as the dopant concentration increases from 0 to 1×10^{18} cm^{-3} and to 5×10^{18} cm^{-3}.

The data shown in Table I are plotted in Fig. 2 for representative samples, showing the free electron concentration, mobility, and conductivity of Si-doped $Al_xGa_{1-x}N$ alloys (of three different Al contents, $x=0.4$, 0.45, and 0.5) versus Si dopant concentrations N_{Si}. In resonance with the PL data shown in Fig. 1, we see that the electrical properties also improve significantly with Si doping. Most importantly, Fig. 2 reveals that there exists a critical Si-dopant concentration for converting insulating $Al_xGa_{1-x}N$ ($x\geqslant 0.4$) to *n*-type, and the critical dopant concentration is about 1×10^{18} cm^{-3}.

We have investigated in more detail the influence of the Si dopant concentration on the carrier localization properties in $Al_xGa_{1-x}N$ alloys. This was accomplished by measuring the thermal activation energy of the PL emission intensity and the PL recombination lifetime as functions of Si dopant concentration. Figure 3 shows the Arrhenius plots of PL emission intensity of $Al_{0.45}Ga_{0.55}N$ epilayers with different Si dopant concentrations. The solid lines in Fig. 3 are the least square fits of data with the standard equation that describes the thermal activation energy of the PL emission intensity:[11]

$$I_{emi}(T)=I_0/[1+C\exp(-E_0/kT)], \tag{1}$$

where E_0 is the thermal activation energy of the PL emission intensity, which measures the effective carrier localization energy in this case. The fitted activation energies E_0 are also indicated in Fig. 3. Figure 4(a) shows temporal responses of the PL emission of $Al_{0.45}Ga_{0.55}N$ samples with three different Si dopant concentrations measured at their respective spectral peak positions. It clearly shows a systematic decrease of the recombination lifetime with increasing N_{Si}.

The recombination lifetime τ and activation energy E_0 of the PL emission intensity for $Al_{0.45}Ga_{0.55}N$ epilayers as functions of Si dopant concentration are plotted in Fig. 4(b), which shows that τ and E_0 follow the same trend. Both values of τ and E_0 exhibit initial sharp decreases when the Si dopant concentration is increased from $N_{Si}=0$ to $N_{Si}=1$

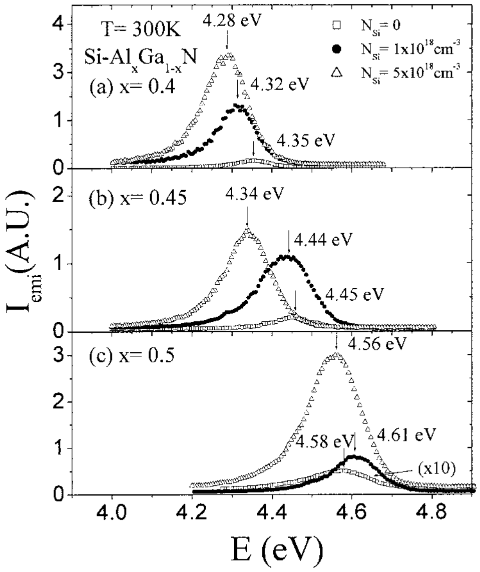

FIG. 1. Room temperature PL spectra of Si-doped $Al_xGa_{1-x}N$ alloys with three different Si dopant concentrations (N_{Si}) for (a) $x=0.4$, (b) $x=0.45$, and (c) $x=0.5$.

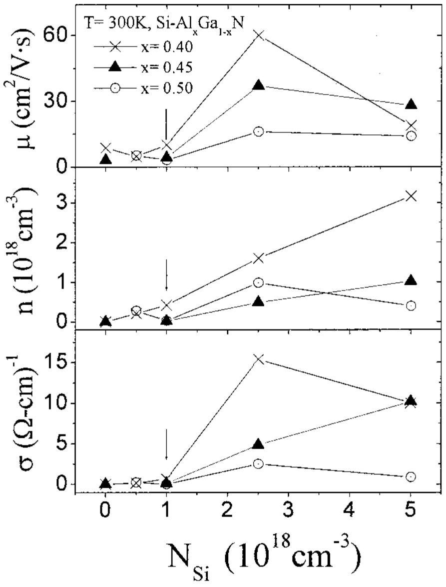

FIG. 2. The free electron concentration (n), mobility (μ), conductivity σ of Si-doped $Al_xGa_{1-x}N$ alloys as functions of the Si dopant concentration (N_{Si}) for three different Al compositions, $x=0.4$, 0.45, and 0.5.

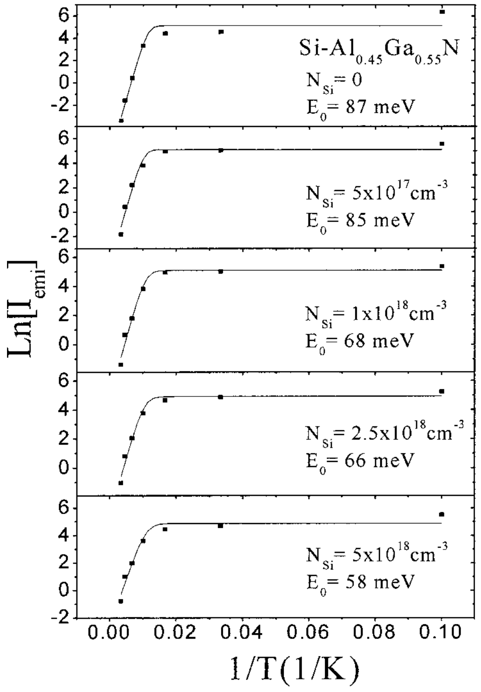

FIG. 3. The Arrhenius plot of the integrated PL emission intensity (I_{emi}) for Si-doped $\mathrm{Al}_{0.45}\mathrm{Ga}_{0.55}\mathrm{N}$ alloy with different Si dopant concentrations. The solid lines are the least square fits of data with Eq. (1). The fitted activation energies E_0 are also indicated in the figure for different Si dopant concentrations.

$\times 10^{18}$ cm^{-3}, followed by gradual decreases as N_{Si} further increases. These results thus suggest that Si-doping reduces the carrier localization energy and that a sharp reduction in effective carrier localization energy occurs at around $N_{\mathrm{Si}} = 1\times 10^{18}$ cm^{-3}. The results shown in Fig. 4(b) thus corroborate the electrical data presented in Table I and in Fig. 2. Therefore, one must fill up the localization states before the carriers could transport via extended states and reasonable *n*-type conductivities could be achieved, while the critical Si-dopant concentration needed to do this is around $N_{\mathrm{Si}} = 1\times 10^{18}$ cm^{-3}.

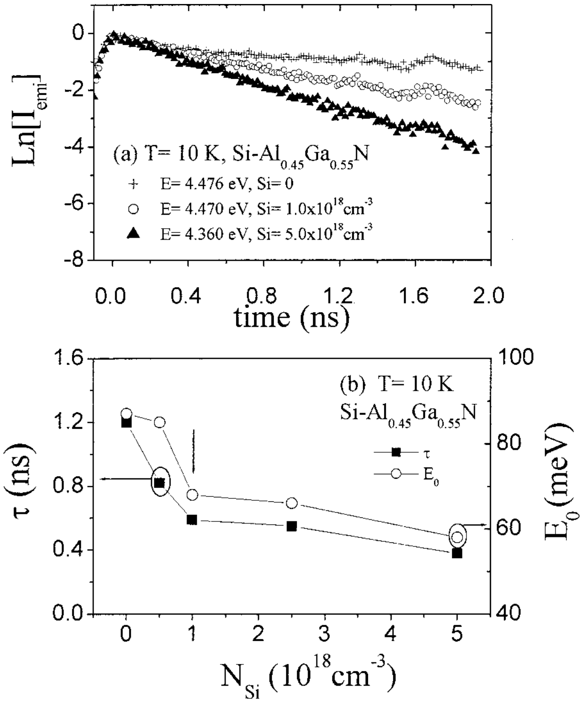

FIG. 4. (a) Temporal responses of PL emission of Si-doped $\mathrm{Al}_{0.45}\mathrm{Ga}_{0.55}\mathrm{N}$ alloy for three different Si dopant concentrations (N_{Si}). (b) Si dopant concentration dependence of the recombination lifetime τ and thermal activation energy E_0 of the PL emission intensity for $\mathrm{Al}_{0.45}\mathrm{Ga}_{0.55}\mathrm{N}$ alloys.

TABLE II. Hall data of Si-doped $\mathrm{Al}_x\mathrm{Ga}_{1-x}\mathrm{N}$ ($0.3\leq x\leq 0.5$): Improved results for Si dopant concentration $N_{\mathrm{Si}}=5\times 10^{18}$ cm^{-3}

	x			
	0.5	0.6	0.65	0.7
	KSU-A597	KSU-A595	KSU-A594	KSU-A599
$\sigma(\Omega\,\mathrm{cm})^{-1}$	8.3	6.7	6.7	2.2
$\mu(\mathrm{cm}^2/\mathrm{Vs})$	33.6	30	20	21
$n(\mathrm{cm}^{-3})$	1.44×10^{18}	1.9×10^{18}	2.1×10^{18}	6.2×10^{17}

Indeed, by fixing the Si dopant concentration at 5×10^{18} cm^{-3} while varying the growth conditions slightly, we have achieved highly conductive $\mathrm{Al}_x\mathrm{Ga}_{1-x}\mathrm{N}$ alloys with high Al content (*x* up to 0.7). The Hall data for this new batch of samples are summarized in Table II. Conductivity values of 6.7 and 2.2 Ω^{-1}cm^{-1}, respectively, have been achieved for $\mathrm{Al}_{0.65}\mathrm{Ga}_{0.35}\mathrm{N}$ and $\mathrm{Al}_{0.7}\mathrm{Ga}_{0.3}\mathrm{N}$ alloys.

In summary, we have investigated the growth, optical, and electrical properties of Si-doped $\mathrm{Al}_x\mathrm{Ga}_{1-x}\mathrm{N}$ alloys with *x* up to 0.7. Our results revealed that (i) the conductivity of Si-doped $\mathrm{Al}_x\mathrm{Ga}_{1-x}\mathrm{N}$ alloys increases with the Si dopant concentration (N_{Si}), and a sharp increase occurs around $N_{\mathrm{Si}}=1\times 10^{18}$ cm^{-3} and (ii) high conductivity can be achieved for *x* up to 0.7 by Si doping. In III-nitride visible emitters, the typical *n*-type conductivity of Si-doped GaN is around 300 Ω^{-1}cm^{-1} and the *p*-type conductivity of Mg-doped GaN is around 1 Ω^{-1}cm^{-1}. We believe that the *n*-type conductivity values we have achieved here for $\mathrm{Al}_x\mathrm{Ga}_{1-x}\mathrm{N}$ alloys (*x* up to 0.7) are sufficiently high for deep UV (~280 nm) emitter applications.

This research is supported by grants from DARPA, BMDO, ARO, ONR, DOE (Grant No. 96ER45604/A000), and NSF (Grant No. DMR-9902431).

[1] H. Morkoc, S. Sstrite, G. B. Gao, M. E. Lin, B. Sverdlov, and M. Burns, J. Appl. Phys. **76**, 1363 (1994).
[2] S. N. Mohammad, A. A. Salvador, and H. Morkoc, Proc. IEEE **83**, 1306 (1995).
[3] J. Li, K. B. Nam, J. Y. Lin, and H. X. Jiang, Appl. Phys. Lett. **79**, 3245 (2001).
[4] C. Skierbiszeski, T. Suski, M. Leszczynski, M. Shin, M. Skowronski, M. D. Bremser, and R. F. Davis, Appl. Phys. Lett. **74**, 3833 (1999).
[5] V. Adivarahan, G. Simin, G. Tamulaitis, R. Srinivasan, J. Yang, and M. Asif Khan, Appl. Phys. Lett. **79**, 1903 (2001).
[6] Internet address http://www.phys.ksu.edu/area/GaNgroup
[7] X. Zhang, S.-J. Chua, W. Liu, and K.-B. Chong, Appl. Phys. Lett. **72**, 1890 (1998).
[8] Z. Q. Li, H. Chen, H. F. Liu, L. Wan, M. H. Zhang, Q. Juang, and J. M. Zhou, Appl. Phys. Lett. **76**, 3765 (2000).
[9] S. Ruvimov, Z. Liliental-Weber, T. Suski, J. W. Ager III, and J. Washburn, Appl. Phys. Lett. **69**, 990 (1996).
[10] K. C. Zeng, J. Y. Lin, H. X. Jiang, A. Salvador, G. Popovici, H. Tang, W. Kim, and H. Morkoc, Appl. Phys. Lett. **71**, 1368 (1997).
[11] J. I. Pankove, *Optical Processes in Semiconductors* (Dover, New York, 1971).